

This discussion paper is/has been under review for the journal Biogeosciences (BG).
Please refer to the corresponding final paper in BG if available.

Influences of tidal energy advection on the surface energy balance in a mangrove forest

J. G. Barr¹, J. D. Fuentes², M. S. DeLonge³, T. L. O'Halloran⁴, D. Barr⁵, and J. C. Ziemann⁵

¹South Florida Natural Resource Center, Everglades National Park, Homestead, FL, USA

²Department of Meteorology, The Pennsylvania State University, University Park, PA, USA

³Department of Environmental Science, Policy, and Management, University of California, Berkeley, CA, USA

⁴Department of Environmental Studies, Sweet Briar College, Sweet Briar, VA, USA

⁵Department of Environmental Sciences, University of Virginia, Charlottesville, VA, USA

Received: 25 July 2012 – Accepted: 2 August 2012 – Published: 30 August 2012

Correspondence to: J. G. Barr (jordan_barr@nps.gov)

Published by Copernicus Publications on behalf of the European Geosciences Union.

BGD

9, 11739–11765, 2012

Influences of tidal energy advection on the surface energy balance

J. G. Barr et al.

Title Page

Abstract

Introduction

Conclusions

References

Tables

Figures

⏪

⏩

◀

▶

Back

Close

Full Screen / Esc

Printer-friendly Version

Interactive Discussion

Abstract

Mangrove forests are ecosystems susceptible to changing water levels and temperatures due to climate change as well as perturbations resulting from tropical storms. Numerical models can be used to project mangrove forest responses to regional and global environmental changes, and the reliability of these models depends on surface energy balance closure. However, for tidal ecosystems, the surface energy balance is complex because the energy transport associated with tidal activity remains poorly understood. This study aimed to quantify impacts of tidal flows on energy dynamics within a mangrove ecosystem. To address the research objective, an intensive study was conducted in a mangrove forest located along the Shark River in the Everglades National Park, FL. Forest-atmosphere energy exchanges were quantified with an eddy covariance system deployed on a flux tower. The lateral energy transport associated with tidal activity was calculated based on a coupled mass and energy balance approach. The mass balance included tidal flows and accumulation of water on the forest floor. The energy balance included temporal changes in enthalpy, resulting from tidal flows and temperature changes in the water column. By serving as a net sink or a source of available energy, tidal flows reduced the impact of high radiational loads on the mangrove forest. Including tidal energy advection in the surface energy balance improved the 30-min daytime energy closure from 73 % to 82 % over the study period. Also, the cumulative sum of energy output improved from 79 % to 91 % of energy input during the study period. Results indicated that tidal inundation provides an important mechanism for heat removal and that tidal exchange should be considered in surface energy budgets of coastal ecosystems. Results also demonstrated the importance of including tidal energy advection in mangrove biophysical models that are used for predicting ecosystem response to changing climate and regional freshwater management practices.

Influences of tidal energy advection on the surface energy balance

J. G. Barr et al.

Title Page

Abstract

Introduction

Conclusions

References

Tables

Figures



Back

Close

Full Screen / Esc

Printer-friendly Version

Interactive Discussion



1 Introduction

Despite their ecological importance, coastal ecosystems remain largely under-studied for their capacity to store carbon and cycle energy. For example, the fringe mangrove forests in the Florida Everglades provide a wide range of ecosystem services for local fisheries (Odum and Heald, 1972; Odum et al., 1982) and atmospheric carbon dioxide assimilation (Barr et al., 2010, 2012). Their pan-tropical distribution and continuous growing season permit mangrove forests to exhibit unique carbon and energy cycling patterns (Barr et al., 2010). To fully understand and quantify forest-atmosphere carbon and water vapor exchanges, it is necessary to ascertain the mechanisms and time scales of energy flows through forested systems (Wilson et al., 2002). In mangrove forests, the flow of water during flood and ebb tides may substantially influence the energy transport within the canopy. In terrestrial ecosystems, available energy represents the difference between net radiation (R_{net}) and the flux of heat into or out of the soil (G). Neglecting energy stored in the biomass, the available energy ($R_{net} - G$) is then partitioned into sensible (H) and latent heating (LE) in the vertical direction. In tidal settings, water inundating the forest floor stores or releases energy as well as carries energy to and from adjacent estuaries. The energy exchange that occurs during flood and ebb tidal cycles must be incorporated into the surface energy budget.

Limited studies have attempted to quantify energy flows in coastal landscapes affected by variable surface water levels. Heilman et al. (1999, 2000) used conditional eddy-covariance and Bowen ratio methods to determine the components of the surface energy balance of a coastal marsh near Corpus Christi, TX. Their results showed a poor closure of the surface energy balance that depended on surface water levels and exhibited a strong seasonal signal. Annual energy fluxes revealed that the marsh functioned more like a dryland ecosystem, with enhanced latent heat prevailing in the spring during the highest water levels and greatest sensible heat in the summer. In the coastal environment, a clear relationship existed between surface water levels and energy flows. Also, Hogue et al. (1999) utilized conservation of mass and heat flow

BGD

9, 11739–11765, 2012

Influences of tidal energy advection on the surface energy balance

J. G. Barr et al.

Title Page

Abstract

Introduction

Conclusions

References

Tables

Figures



Back

Close

Full Screen / Esc

Printer-friendly Version

Interactive Discussion



equations to estimate temperature and salt dynamics of the Ponta Rasa mangrove swamp in Mozambique. The Ponta Rasa system, which exhibited a twice-daily tide component, was divided into two reservoirs: the Maputo Bay and the mangrove swamp. Results indicated that heat and salt were laterally transported in narrow channels connecting the reservoirs.

In the tidally influenced mangrove forests of the Everglades, FL, USA estuarine waterways flow southwest to the Gulf of Mexico and flood the forest floor up to two times a day (Fig. 1). During low tides in the summer, the water is cooler than the overlying air in the afternoon, and the receding water transports heat away from the forest floor to the adjacent estuary. The physical process of heat transfer occurs as the cool water contacts warmer soils below and air above during flood tide periods. During these periods most of the energy exchange occurs across the soil-water and water-atmosphere interfaces at points of water entry into the mangrove forest (the mangrove-estuary interface) and along the sediment-water and water-atmosphere interfaces as the tidal waters penetrate into the forest. These unique energy exchange processes have not been previously explored in coastal systems. It is necessary to understand these energy flows because their temporal variability has implications for fluctuations in soil and air temperature, which influence net ecosystem carbon exchange (NEE) over daily and annual time scales (Barr et al., 2012; Ito et al., 2005; van Dijk et al., 2005).

This study aimed to determine the heat flux into the water inundating the soil surface to improve energy budgets for the tidally influenced mangrove forest by accounting for both (i) lateral advection of energy at the forest-estuary interface and (ii) vertical exchanges of energy at the water-soil and water-atmosphere interfaces. We estimated the vertical transport of energy at the forest-atmosphere interface and the lateral advection of energy by computing the temporal changes in enthalpy of floodwaters during residence within the flux footprint of an eddy covariance (EC) tower. Results were used to understand the mechanics of tidal energy flows and the magnitude of these in relation to vertical exchanges of latent and sensible heat. This work represents a first step toward understanding how tidal energy exchange affects the mangrove microclimate

Influences of tidal energy advection on the surface energy balance

J. G. Barr et al.

Title Page

Abstract

Introduction

Conclusions

References

Tables

Figures



Back

Close

Full Screen / Esc

Printer-friendly Version

Interactive Discussion



and the consequential influences on physiological processes including photosynthesis and water use efficiency.

2 Site description

Located mostly within the boundaries of Everglades National Park (ENP), mangroves represent the dominant primary producers within the coastal Florida Everglades and extend over 1.75×10^7 ha (Lugo et al., 1975). The ENP includes over 4.3×10^5 ha of the Everglades watershed, which is one of the largest freshwater wetland landscapes in North America. The study site was located within a riverine mangrove forest along Shark River (Fig. 1), adjacent to the Florida Coastal Everglades Long-Term Ecological Research (FCE-LTER) site 6 in Shark River Slough (SRS6) (25.36462994° N, 81.07794623° W). Red (*Rhizophora mangle*), white (*Languncularia racemosa*), and black (*Avicennia germinans*) mangroves dominate the forest and form a reasonably closed and continuous canopy. The foliage distribution is confined from about 10 m above the surface to the canopy top (15 m on average). The sparse forest understory is comprised primarily of seedlings and juvenile red mangrove trees whose average height is less than 4 m. Compact sediments and the mangrove rooting system are confined from the surface to 1 m below ground and are flooded with 0.5 m of water during high tides. The wetland peat is up to 6 m thick and is underlain by limestone bedrock. The topography is flat and largely governed by tidal creeks that penetrate the forest. The field study was carried out during 6–16 August 2005.

3 Research methodology

3.1 Energy balance components

Energy fluxes and meteorological conditions were quantified based on measurements made from a flux tower, which was located approximately 250 m inland from the edge

BGD

9, 11739–11765, 2012

Influences of tidal energy advection on the surface energy balance

J. G. Barr et al.

Title Page

Abstract

Introduction

Conclusions

References

Tables

Figures

◀

▶

◀

▶

Back

Close

Full Screen / Esc

Printer-friendly Version

Interactive Discussion



Influences of tidal energy advection on the surface energy balance

J. G. Barr et al.

Title Page

Abstract

Introduction

Conclusions

References

Tables

Figures

⏪

⏩

◀

▶

Back

Close

Full Screen / Esc

Printer-friendly Version

Interactive Discussion



of Shark River. An eddy covariance system was used to calculate fluxes of sensible (H) and latent (LE) heat transported across the forest-atmosphere interface (Fig. 2). Vertical wind velocity and temperature were measured at 10 Hz with a 3-dimensional sonic anemometer (model RS-50, Gill Co., Lymington, England) mounted at 27 m. An adjacent open path infrared gas analyzer (Li-7500, LI-COR Inc., Lincoln, NE) measured water vapor concentration at 10 Hz. These measurements were processed with custom-made software to derive half-hourly fluxes of H , LE, carbon dioxide (CO_2), and momentum exchanges between the forest and overlying atmosphere (Barr et al., 2010). Software data processing includes spike removal (Vickers and Mahrt, 1997), buoyancy corrections of sonic air temperatures (Schotanus et al., 1983), and calculation of the total constituent flux (Webb et al., 1980) which accounts for positive vertical mass flow resulting from buoyancy of less dense air parcels. Relative humidity at 27 m was calculated with measurements from a ventilated thermistor-hygistor probe. A net radiometer (Model CNR 1, Kipp and Zonen, Bohemia, NY) recorded net radiation (R_{net}). Heat flux plates (model HFT 3.1, Campbell Scientific, Logan, UT) were placed at 0.1 m below the sediment surface measured the direction and magnitude of energy flow (G) through the soil. In terrestrial ecosystems, the soil serves as a capacitor for heat, whereby heat is stored during the daytime and released to the atmosphere during the nighttime. However, in mangrove ecosystems, the lateral advection of enthalpy (ΔH_{adv}) describes the amount of energy stored (or released) from the water column and exchanged with the estuary during flood and ebb tides. The magnitude of ΔH_{adv} is controlled by four distinct processes: (i) heat transfer (conduction) between the sediment and overlying water column, (ii) heat conduction between the water column and the overlying atmosphere, (iii) evaporation at the water-atmosphere interface (removing heat from the water column), and (iv) direct absorption of solar irradiance by the water column. During ebb tides, enthalpy is transferred from the water inundating the surface into the surrounding estuary, which is outside of the tower flux footprint contributing to H and LE (Fig. 2). The surface energy balance can then defined as

$$R_{\text{net}} - G - S = H + \text{LE} + \Delta H_{\text{adv}} \quad (1)$$

where S includes energy required to heat (or cool) above ground biomass and air between the surface and 27 m and chemical energy stored during photosynthesis (Gu et al., 2007). A positive value of S indicates storage of energy within the ecosystem during the time interval (30 min) and contributes to lowering of the energy available for partitioning into sinks. The magnitude of S can be important ($\sim 5\%$ of R_{net}) during short (30 min) time intervals. However, when components of the energy budget are integrated over time periods of a day or more, S is generally negligible ($< 5\%$ of R_{net}) compared to the other source and sink terms. This simplification provides the energy budget used in this study (Fig. 2),

$$R_{\text{net}} - G = H + \text{LE} + \Delta H_{\text{adv}} \quad (2)$$

Closure of the surface energy budget was determined as the slope of the least-squares regression line forced through the origin of daytime half-hourly available energy ($R_{\text{net}} - G$) versus energy sink terms in Eq. (2) during the 10-day study period. The analysis was performed separately by both including and excluding ΔH_{adv} as one of the sink terms along with H and LE. To account for the possibility that the time scales of energy sinks were not exactly synchronized with available energy input, cumulative daytime fluxes of ($R_{\text{net}} - G$), ($H + \text{LE}$) and ($H + \text{LE} + \Delta H_{\text{adv}}$) in MJ m^{-2} were determined. Energy closure was estimated as the ratio of the cumulative energy sink, with and without ΔH_{adv} included, to cumulative available energy at the end of the study period.

3.2 Estimation of lateral energy fluxes

We quantified lateral energy advection by tides at the study site (Fig. 1) by considering mass and energy budgets for water similar to Hogue et al. (1999). To obtain spatially accurate temperature and water level gradients, the study site was partitioned into four rectangular sectors, A through D (Fig. 3). Three independently instrumented locations (Sites 1–3; Fig. 3) were established along a transect extending from the edge of Shark River to the flux tower (~ 250 m). As in previous studies (Heilman et al., 2000), heat fluxes into or out of the soil were determined at each site using heat flux plates (model

BGD

9, 11739–11765, 2012

Influences of tidal energy advection on the surface energy balance

J. G. Barr et al.

Title Page

Abstract

Introduction

Conclusions

References

Tables

Figures

⏪

⏩

◀

▶

Back

Close

Full Screen / Esc

Printer-friendly Version

Interactive Discussion



HFT 3.1 Heat Flux Plates, Campbell Scientific Inc., Logan, UT) buried 0.1 m below the sediment surface. Spatially averaged soil heat flux including the 3 sites was used to represent G in Eq. (2) in place of the measurements adjacent to the tower. Measurements included periods when the soil was exposed and inundated during flood tides. At each site, water temperature was measured with three type E thermocouples (*Omega Engineering*, Inc., Stamford, CT) deployed at different heights (0.05, 0.13, and 0.31 m) above the soil surface. A water level sensor (model WL400, Global Water Instrumentation, Inc., Gold River, CA) provided water depth at each site, which was used to identify periods when thermocouples were exposed to the atmosphere. Within the mouth of the tidal creek, E-type thermocouples were also deployed at 0.05, 0.13, and 0.31, and 0.51 m. Flow velocity in the creek was measured with a flow meter (model Flo-Tote 3, Marsh McBirney, Frederick, MD). Point measurements of velocity were converted to depth- and width-averaged velocity (U ; in m s^{-1}). Water level, measured by the flow meter's pressure transducer, along with user specified information of the channel geometry, was used to compute instantaneous cross-sectional area, A (in m^2). Recharge quantities (Q ; in $\text{m}^3 \text{min}^{-1}$) entering (exiting) the tidal creek from Shark River was determined as 10-min averages as

$$Q = \left[\int_{t=0}^{600s} (UA) dt \right] / 10 \text{ min} \quad (3)$$

Water temperature (\overline{T}_i) in sectors A–D (Fig. 3) were determined by assuming a linear temperature gradient between each site and solving for the temperature at the midpoint of each sector along a transect connecting the sites. Water temperatures were vertically and temporally averaged at each site and included only those measurements when thermocouples were submerged. The ΔH_{adv} (W m^{-2}) was determined as the change in enthalpy storage (ΔH_{stor}) of water inundating the surface and contributions from flow entering ($H_{\text{in}} > 0$) or exiting ($H_{\text{in}} < 0$) the forest via the adjacent river divided by the time interval, Δt (i.e., 10 min (600 s)) over which the change occurred.

$$\Delta H_{\text{adv}} = (\Delta H_{\text{stor}} - H_{\text{in}}) / \Delta t \quad (4)$$

BGD

9, 11739–11765, 2012

Influences of tidal energy advection on the surface energy balance

J. G. Barr et al.

Title Page

Abstract

Introduction

Conclusions

References

Tables

Figures

◀

▶

◀

▶

Back

Close

Full Screen / Esc

Printer-friendly Version

Interactive Discussion



The ΔH_{stor} (W m^{-2}) is the difference in enthalpy storage between the current period ($H_{\text{stor},i}$) and the previous one ($H_{\text{stor},i-1}$) during the time interval, Δt . At each time step, H_{stor} was determined as,

$$H_{\text{stor}} = \frac{\sum_{j=1}^n \rho C_w h_j A_j T_j}{\sum_{j=1}^n A_j} \quad (5)$$

5 where ρ is the density of water (kg m^{-3}) and C_w is the specific heat capacity of water ($4186 \text{ J kg}^{-1} \text{ C}^{-1}$). The h_j , A_j , and T_j are water depth (m), area (m^2), and average water temperature (C), respectively, within each sector j . The total drainage area of the tidal creek ($A_{\text{tot}} = \sum_{j=1}^n A_j$) was determined from linear least-squares regression of the flow entering (exiting) the tidal creek during each 10 min interval versus the change in the sum of cross sectional area of water inundating the surface in all four sectors. During flood and ebb tide periods, when the soil was inundated, the slope of the regression provided an estimate of the width (w) of the creek drainage perpendicular to the creek axis and the line connecting the 3 sites and tower. This width was then used to estimate the rectangular area of each sector (Fig. 3) and the change in volume resulting from flow through the tidal creek. During tidal inflows (outflows), the enthalpy entering (exiting) the forest through the tidal creek was estimated as,

$$H_{\text{in}} = \frac{\Delta V \rho C_w \overline{T}_{\text{cr}}}{A_{\text{tot}} \Delta t} \quad (6)$$

where ΔV (m^3) is the total volume change during time interval, Δt (s), in all four sectors, and \overline{T}_{cr} (C) is the average water temperature entering (exiting) the mouth of the tidal creek. During ebb tide ($\Delta V < 0$), and energy is exiting the forest ($H_{\text{in}} < 0$ in Eq. 6).

Influences of tidal energy advection on the surface energy balance

J. G. Barr et al.

Title Page

Abstract

Introduction

Conclusions

References

Tables

Figures

⏪

⏩

◀

▶

Back

Close

Full Screen / Esc

Printer-friendly Version

Interactive Discussion



During the end of ebb tide, the water level in the creek dropped below 0.05 m and the enthalpy exported to the estuary was estimated as,

$$H_{in} = \sum_{j=1}^n \frac{\Delta V_j \rho C_w \bar{T}_j}{A_j \Delta t} \quad (7)$$

where ΔV_j (m^3) is the change in volume within each sector. During these periods, water inundating the surface was also likely exported through seepage in the sediment, overbank flow, and flow through the tidal creek. Any additional heat transfer that may have occurred as the water flowed through the sediment and into the tidal creek or river banks was not measured and was therefore not included in this analysis. However, when water levels were high (> 0.05 m above the surface) the flow through tidal creeks was the primary mechanism for export of water and enthalpy into the adjacent river. Recharge was not used in determining import and export of enthalpy since the analysis required mass balance closure.

4 Results and discussion

4.1 Radiation loads and energy partitioning

Limited information exists on long-term ($>$ months) sensible and latent heat fluxes for tidally influenced mangroves. To determine whether forest-atmosphere energy changes exhibit different patterns during high and low tides, averaged fluxes were estimated for seasonal periods similar to the ones included in the 10-day study. During July to September 2004 and July and August 2005, average midday (12:00–14:00 h) R_{net} (Fig. 4a) was higher during low tide periods (535–640 $W m^{-2}$) compared to high (525–560 $W m^{-2}$) tide periods. These trends contributed to increased midday H (Fig. 4b) during high (H of 150–180 $W m^{-2}$) compared to low tide (H of 125–140 $W m^{-2}$) periods. Average midday LE (Fig. 4c) was also higher during low (LE of 250–315 $W m^{-2}$)

Influences of tidal energy advection on the surface energy balance

J. G. Barr et al.

Title Page

Abstract

Introduction

Conclusions

References

Tables

Figures

⏪

⏩

◀

▶

Back

Close

Full Screen / Esc

Printer-friendly Version

Interactive Discussion



compared to high tide (LE of 225–265 W m⁻²) periods. While the magnitudes of midday H and LE were mostly controlled by R_{net} , the partitioning of energy into H and LE was weakly controlled by tidal inundation status. Diurnal average H/R_{net} and LE/R_{net} ratios (data not shown) were 7% to 13% and -4% to 15% higher, respectively, comparing low to high tides during 12:00 to 15:00 h. Soil heat flux adjacent to the tower (Fig. 4d) was $\sim 5 \text{ W m}^{-2}$ higher comparing low to high tides during 13:00 to 15:00 h. During daytime hours, the soil was a weak source of energy (-7 to 2 W m^{-2} , on average) in the morning (07:00 to 10:00 h) and a weak sink of energy (2 to 16 W m^{-2} , on average) during the afternoon (12:00 to 18:00 h), regardless of inundation. These results suggest that tidal flows provided an additional sink of energy during the warm summer months of July to September.

4.2 Water flow dynamics and tidal energy advection

Although topographic changes in the mangrove forest landscape were slight (1 m or less), the differences strongly affected the flow dynamics at the study site. Flow dynamics are illustrated by the time series of water level on the forest floor at three sites (Fig. 5a) and within the tidal creek (Fig. 5b). Tidal fluctuations were highly asymmetrical during incoming and outgoing tide. During flood tide, water levels increased rapidly as water was forced through the tidal creek. However, during ebb tide, the flow of water was resisted by soil roughness, the presence of pneumatophores, and obstacles such as coarse woody debris and leaf litter. This reduction in flow was most evident in the inflection in water levels at sites 2 and 3 that occurred as levels dropped below about 0.1 m. Within these ebb tide periods, a fraction of water percolated through the soil and returned to the river through lateral subsurface flow rather than exiting directly through the tidal creek. Subsurface flow was also evidenced by asymmetric recharge through the tidal creek (Fig. 5c). Flow entering through the creek (i.e., recharge) was visible during each flood tide, but discharge of water exiting the creek during ebb tides was substantially dampened and in some cases not observed. The width of the creek

BGD

9, 11739–11765, 2012

Influences of tidal energy advection on the surface energy balance

J. G. Barr et al.

Title Page

Abstract

Introduction

Conclusions

References

Tables

Figures

⏪

⏩

◀

▶

Back

Close

Full Screen / Esc

Printer-friendly Version

Interactive Discussion

drainage was estimated as 340 m as determined from the slope of the regression line of flow through the creek versus change in cross sectional area in the four sectors. This large (340 m) drainage width provided some context for the asymmetry in creek discharge observed during ebb tide periods.

5 The timing of tidal flows and inundation (Fig. 5) in relation to available energy represented a key control on the direction and magnitude of tidal energy advection. On 13 August 2005, floodwaters were initially a source of energy to the forest in the morning ($\Delta H_{adv} = -165 \text{ W m}^{-2}$ at 08:30 h; Fig. 6a) when inundation was greatest (Fig. 6b). During ebb tides, when water drained from the forest floor (09:30 to 13:30 h), the receding waters were a sink for available energy (up to 320 W m^{-2}). Higher air temperature and positive available energy (not shown) resulted in air-water heat transfer and direct warming of the water column from absorption of solar irradiance. Diurnal patterns in H and LE on 13 August (Fig. 6a) were representative of energy exchange rates observed during the 10-day study period. Daytime LE exceeded H by a ratio of roughly 2 : 1. 10 Temporal patterns in soil heat flux were comparable at the tower and averaged for the 3 sites (G tower, Fig. 6a). The soil served as a weak sink for energy (G of $5\text{--}17 \text{ W m}^{-2}$) during the daytime and a weak source of energy (G of -10 to 0 W m^{-2}) during nighttime hours.

Ensemble averages of energy source and sink terms (Fig. 7) were used to understand the role of tidal energy advection in the surface energy budget during the 10-day study period when the forest was flooded. The R_{net} (Fig. 7a) was highest ($580\text{--}810 \text{ W m}^{-2}$) during 12:30 h coincident with peak solar irradiance levels (not shown). Both H and LE (Fig. 7b and c) peaked prior to the maximum R_{net} at 11:30 h (H of $120\text{--}200 \text{ W m}^{-2}$) and 11:00 h (LE of $230\text{--}480 \text{ W m}^{-2}$), respectively. Both H and LE exhibited secondary peaks of 140 W m^{-2} and 245 W m^{-2} (ensemble averages), respectively, at 15:30 h. These midday troughs in ensemble average H and LE were attributed to the increasing energy advection of tidal waters (Fig. 7d) from an average of 5 W m^{-2} at 7:00 h to 160 W m^{-2} at 12:30 h. Later in the day, from 14:00 to 17:30 h, flood waters were a source of energy, with ΔH_{adv} reaching a minimum of -125 W m^{-2} at 16:00 h.

Influences of tidal energy advection on the surface energy balance

J. G. Barr et al.

Title Page

Abstract

Introduction

Conclusions

References

Tables

Figures

◀

▶

◀

▶

Back

Close

Full Screen / Esc

Printer-friendly Version

Interactive Discussion



This shift in average ΔH_{adv} during the afternoon from a sink to a source of energy mostly drove the secondary peaks in H and LE. Soil heat flux trends played a minor role compared to ΔH_{adv} in controlling diurnal energy partitioning into H and LE with maximum values of 11–18 W m⁻² (average ± 1 s.d.) at 13:30 h.

Though diurnally variable, tidal energy advection provided a net sink for energy during the 10-day study period. However, the sign and the magnitude of ΔH_{adv} over the course of seasonal cycles likely varied with changes in the temperature gradients between the atmosphere and the floodwaters entering from the river. Least squares regression (Fig. 8) of half-hourly daytime ΔH_{adv} versus the difference between air temperature (at 27 m) and water temperature (site- and depth- averaged) showed a significant increase ($p < 0.01$) in ΔH_{adv} with increasing temperature gradient (slope = 44.7, intercept = -1.4, $R^2 = 0.25$). This trend indicated that flood tides changed from being a net sink to a net source of energy during seasonal transitions in October–November when air masses in south Florida begin to cool but waters in the Gulf of Mexico remain warm. Also, cold fronts lasting for several days frequent the Everglades during December to March. During these periods, floodwaters from Shark River can be warmer than mid-day conditions and provide a source of heat to the forest. Tidal waters may, therefore, serve to ameliorate extreme microclimatic conditions (associated with extreme heating during the summer or unusual coldness during the winter) within the forest canopy. Extreme microclimatic conditions detrimentally impact leaf physiology and net ecosystem carbon exchange (Barr et al., 2010).

Including the energy transfer associated with tidal activity improved the closure of the surface energy balance in the mangrove forest during 6–16 August 2005. When the ΔH_{adv} was considered in the surface energy budget, energy closure improved from 73% to 82% (Fig. 9a and b, respectively). Therefore, tidally driven floodwaters represented a net sink of energy during the daytime. The regressions between available energy and energy sinks (Fig. 9) may not fully incorporate diurnal patterns in energy closure. For instance, during July to September 2004 and July and August 2005, average energy closure ($\Sigma(R_{net} - G)/\Sigma(H + LE)$, data not shown) was lowest (74%) during

BGD

9, 11739–11765, 2012

Influences of tidal energy advection on the surface energy balance

J. G. Barr et al.

Title Page

Abstract

Introduction

Conclusions

References

Tables

Figures

⏪

⏩

◀

▶

Back

Close

Full Screen / Esc

Printer-friendly Version

Interactive Discussion

Influences of tidal energy advection on the surface energy balance

J. G. Barr et al.

Title Page

Abstract

Introduction

Conclusions

References

Tables

Figures

⏪

⏩

◀

▶

Back

Close

Full Screen / Esc

Printer-friendly Version

Interactive Discussion

midday (12:00 to 14:00 h). Closure was highest (82–88 %) during the morning (09:00 to 10:00 h) and late afternoon (15:30 to 17:00 h), when R_{net} and solar irradiance were lower compared to midday levels. To remove any effect these patterns may have had on energy closure, the energy budget was also determined from daytime cumulative sums of energy input ($R_{\text{net}} - G$) and output (Fig. 10) that did not and did include tidal energy advection ($[H + \text{LE}]$ and $[H + \text{LE} + \Delta H_{\text{adv}}]$, respectively). At the end of the study, cumulative sums of $(H + \text{LE})$ and $(H + \text{LE} + \Delta H_{\text{adv}})$ represented 79 % and 91 % of available energy, respectively (Fig. 10). The cumulative summation method provided the evidence of improved energy closure (79 % and 91 %). Furthermore, regression analyses yielded differences (73 % and 82 %) in the degree of surface energy closure whether ΔH_{adv} was included or excluded as energy sink. The inclusion of ΔH_{adv} as an energy sink improved closure by 9 to 12 %. Therefore, advection of energy by tides should not be ignored for its contribution to surface energy budgets in mangrove forests.

The results for the surface energy balance were consistent with previous findings that showed a lack of energy budget closure of about 20 % for various terrestrial ecosystems (Wilson et al., 2002). Even with the contribution of ΔH_{adv} , the energy budget failed to close based on the regression and cumulative sum methods by 18 % and 9 %, respectively. In the present study, the “missing” energy likely originated from both underestimating sensible and latent heat fluxes (Sakai et al., 2001) and not accounting for heat storage in biomass and biochemical reactions (Gu et al., 2007). The present analysis quantified energy transport occurring in surface waters, which included water inundating the soil surface, flow through the tidal creek, and loss in volume through overland flow. Some net loss of energy likely resulted from subsurface flow and heat exchange with the soil. This subsurface flow did not entirely leave the tidal creeks, but some seeped through interstitial spaces along the steep soil banks lining the adjacent river. In a temperate deciduous forest, Gu et al. (2007) found that biomass heat storage and biochemical energy storage ranged from -50 to 50 W m^{-2} and -3 to 20 W m^{-2} , respectively. The storage terms were positively correlated with R_{net} and, consequently, contributed to a reduction in available energy.

5 Conclusions

Results from the present study showed that energy advection associated with tides in a mangrove forest meaningfully affect the surface energy budget. For the warm periods experiencing high ($\sim 800 \text{ W m}^{-2}$) net radiation loads, flooding waters provided a net sink for energy. During high tides, the cooler water inundated the warmer soils and, during low tides, the dissipated heat in the water column resting on soils was transported to the adjacent river. For the duration of the study period, the average energy advection rates ranged from -273 to 291 W m^{-2} (5th to 95th percentiles). Such energy fluxes substantially exceeded soil heat fluxes whose values ranged from -20 to 27 W m^{-2} (5th to 95th percentile). When the lateral transport of energy was included in the surface energy balance then the closure of the energy budget improved by 9% to 12%. The positive correlation observed between lateral energy transport and air-water temperature differences indicated that flood tides provided a microclimate buffer in the mangrove forest ecosystem. Results suggest that during seasonal transitions to cooler air masses, routinely experienced in the Everglades in October and November, warm waters from the Gulf of Mexico provide a net source of energy (when water temperature exceeds air temperature). In this manner, the tidal flows serves as a conduit to transport energy between mangrove forests and coastal waters.

Acknowledgements. The Jones Everglades Research Fund provided support to establish the flux tower and to instrument adjacent sites. The National Science Foundation also supported this research through the Florida Coastal Everglades Long-Term Ecological Research (awards DBI-0620409 and DEB-9910514).

BGD

9, 11739–11765, 2012

Influences of tidal energy advection on the surface energy balance

J. G. Barr et al.

Title Page

Abstract

Introduction

Conclusions

References

Tables

Figures

⏪

⏩

◀

▶

Back

Close

Full Screen / Esc

Printer-friendly Version

Interactive Discussion



References

- Barr, J. G., Engel, V., Fuentes, J. D. Ziemann, J. C., O'Halloran, T. L., Smith III, T. J., and Anderson, G. H.: Controls on mangrove forest-atmosphere carbon dioxide exchanges in western Everglades National Park, *J. Geophys. Res.-Biogeo.*, 115, G02020, doi:10.1029/2009JG001186, 2010.
- Barr, J. G., Engel, V., Smith III, T. J., and Fuentes, J. D.: Hurricane disturbance and recovery of energy balance, CO₂ fluxes and canopy structure in a mangrove forest of the Florida Everglades, *Agr. Forest Meteorol.*, 153, 54–66, 2012.
- Gu, L., Meyers, T., Pallardy, S. G., Hanson, P. J., Yang, B., Heuer, M., Hosman, K. P., Liu, Q., Riggs, J. S., Sluss, D., and Wullschlegger, S. D.: Influences of biomass heat and biochemical energy storages on the land surface fluxes and radiative temperature, *J. Geophys. Res.*, 112, D02107, doi:10.1029/2006JD007425, 2007.
- Heilman, J. L., Cobos, D. R., Hensch, F. A., Campbell, C. S., and McInnes, K. J.: Tower-based conditional sampling for measuring ecosystem-scale carbon dioxide exchange in coastal wetlands, *Estuaries*, 22, 584–591, 1999.
- Heilman, J. L., Heinsch, F. A., Cobos, D. R., and McInnes, K. J.: Energy balance of a high marsh on the Texas Gulf Coast: Effect of water availability, *J. Geophys. Res.*, 105, 22371–22377, 2000.
- Hoguane, A. M., Hill, A. E., Simpson, J. H., and Bowers, D. G.: Diurnal and tidal variation of temperature and salinity in the Ponta Rasa mangrove swamp, Mozambique, *Estuar. Coast. Shelf S.*, 49, 251–264, 1999.
- Ito, A., Saigusa, N., Murayama, S., and Yamamoto, S.: Modeling of gross and net carbon dioxide exchange over a cool-temperate deciduous broad-leaved forest in Japan: Analysis of seasonal and interannual change, *Agr. Forest Meteorol.*, 134, 122–134, 2005.
- Odum, W. E. and Heald, E. J.: Trophic analysis of an estuarine mangrove community, *B. Mar. Sci.*, 22, 671–738, 1972.
- Odum, W. E., McIvor, C. C., and Smith, T. S.: The ecology of mangroves of South Florida: a community profile, US Fish and Wildlife Service, Office of Biological Services, Washington, DC, FWS/OBS – 81/24, 1982.
- Sakai, R. K., Fitzjarrald, D. R., and Moore, K. E.: Importance of low-frequency contributions to eddy fluxes observed over rough surfaces, *J. Appl. Meteorol.*, 40, 2178–2192, 2001.

Influences of tidal energy advection on the surface energy balance

J. G. Barr et al.

Title Page

Abstract

Introduction

Conclusions

References

Tables

Figures

⏪

⏩

◀

▶

Back

Close

Full Screen / Esc

Printer-friendly Version

Interactive Discussion



Influences of tidal energy advection on the surface energy balance

J. G. Barr et al.

Title Page

Abstract

Introduction

Conclusions

References

Tables

Figures

◀

▶

◀

▶

Back

Close

Full Screen / Esc

Printer-friendly Version

Interactive Discussion



Schotanus, P., Nieuwstadt, F. T. M., and De Bruin, H. A. R.: Temperature measurement with a sonic anemometer and its application to heat and moisture fluctuations, *Bound.-Lay. Meteorol.*, 26, 81–93, doi:10.1007/BF00164332, 1983.

van Dijk, A. I. J. M., Dolman, A. J., and Schulze, E. D.: Radiation, temperature, and leaf area explain ecosystem carbon fluxes in boreal and temperate European forests, *Global Biogeochem. Cy.*, 19, GB2029, doi:10.1029/2004GB002417, 2005.

Vickers, D. and Mahrt, L.: Quality control and flux sampling problems for tower and aircraft data, *J. Atmos. Ocean. Tech.*, 14, 512–526, 1997.

Webb, E. K., Pearman, G. I., and Leuning, R.: Correction of the flux measurements for density effects due to heat and water vapor transfer, *Q. J. Roy. Meteor. Soc.*, 106, 85–100, doi:10.1002/qj.49710644707, 1980.

Wilson, K. B., Goldstein, A., Falge, E., Aubinet, M., Baldocchi, D., Berbigier, P., Bernhofer, C., Ceulemans, R., Dolman, H., Field, C., Grelle, A., Ibrom, A., Law, B. E., Kowalski, A., Meyers, T., Moncrieff, J., Monson, R., Oechel, W., Tenhunen, J., Valentini, R., and Verma, S.: Energy balance closure at FLUXNET sites, *Agr. Forest Meteorol.*, 113, 223–243, 2002.

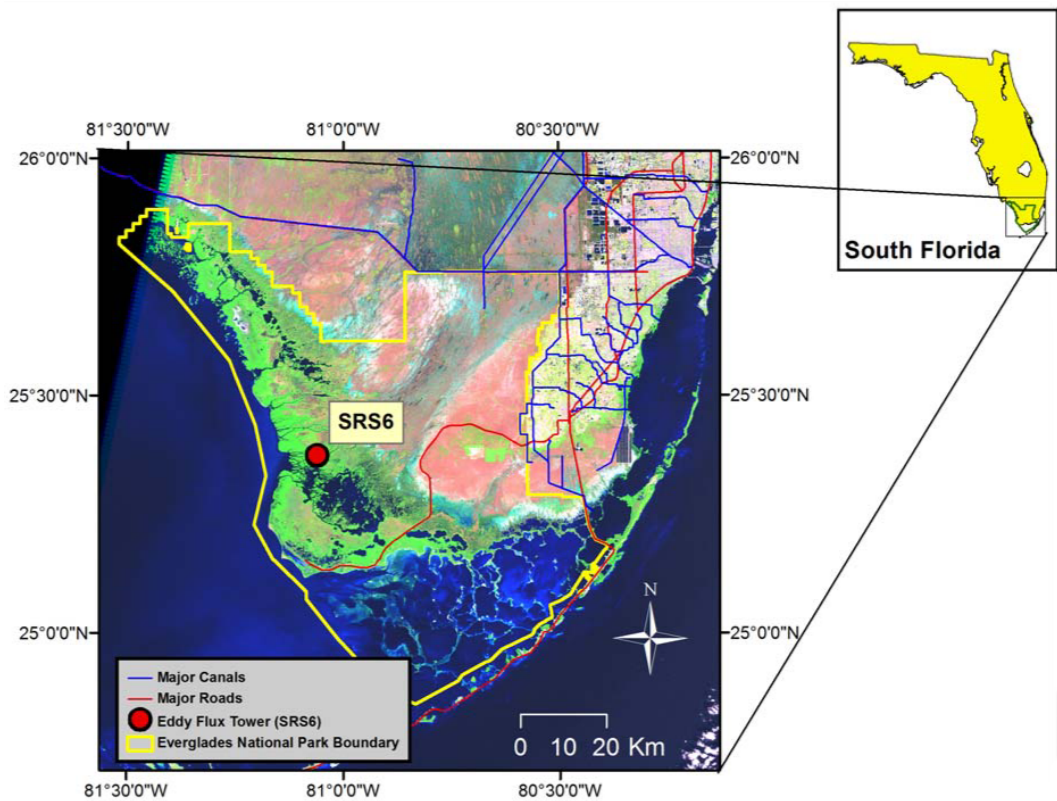


Fig. 1. Landsat 7 thematic map false color composite (RGB bands 5,4,3) of southern Florida including the SRS6 study site and flux tower (site SRS6). Mangrove forests appear as bright green along the southwest coast and southern coast adjacent to the Florida Bay.

Influences of tidal energy advection on the surface energy balance

J. G. Barr et al.

Title Page

Abstract Introduction

Conclusions References

Tables Figures

◀ ▶

◀ ▶

Back Close

Full Screen / Esc

Printer-friendly Version

Interactive Discussion



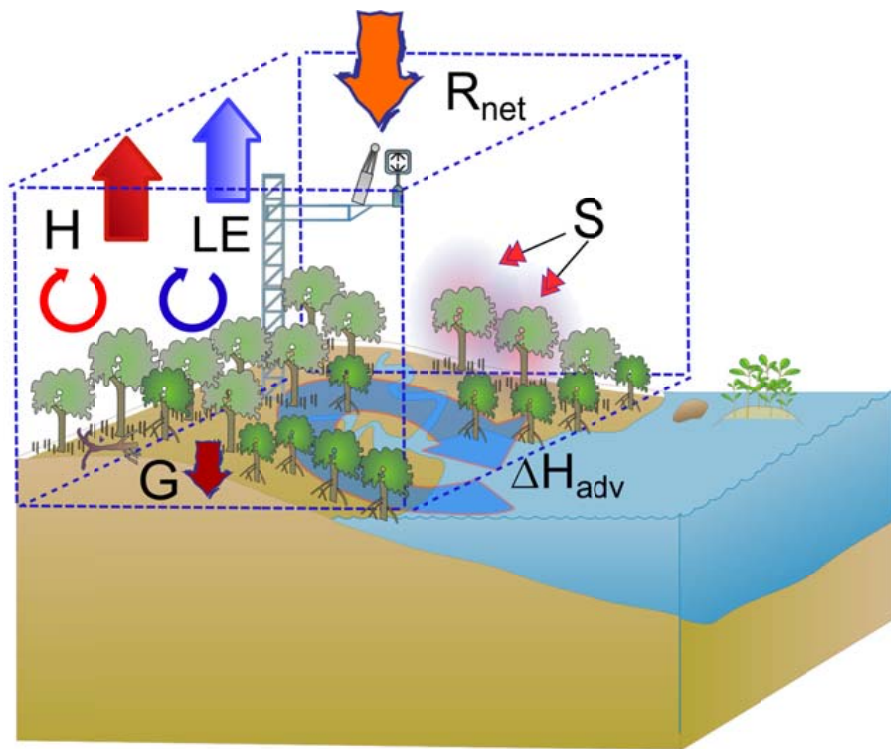


Fig. 2. This conceptual diagram illustrates the key components of the daytime surface energy budget. (When considering the full diel cycles, the fluxes are bidirectional.) The H and LE represent the sensible and latent heat exchanges between the mangrove forest and the atmosphere. The G denotes the heat flow in or out of the soil, and S is the sum of heat and biochemical energy storage in biomass. The ΔH_{adv} is the lateral energy transport to and from the adjacent river and is associated with tidal activity.

Influences of tidal energy advection on the surface energy balance

J. G. Barr et al.

Title Page

Abstract

Introduction

Conclusions

References

Tables

Figures

◀

▶

◀

▶

Back

Close

Full Screen / Esc

Printer-friendly Version

Interactive Discussion



Influences of tidal energy advection on the surface energy balance

J. G. Barr et al.

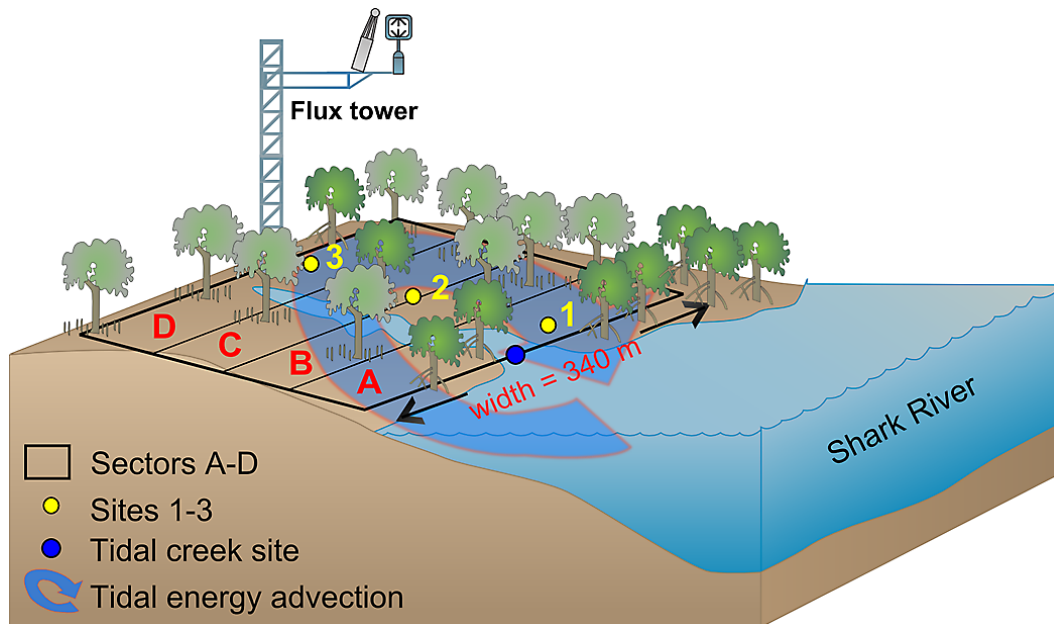


Fig. 3. Conceptual cross section of the study site showing sectors (A–D) each having a width (340 m) perpendicular to the axis of the tidal creek. Inundation level, water temperature, and soil heat flux were measured at sites 1–3. Recharge, water level and temperature were measured within the mouth of the tidal creek site.

Title Page

Abstract

Introduction

Conclusions

References

Tables

Figures

◀

▶

◀

▶

Back

Close

Full Screen / Esc

Printer-friendly Version

Interactive Discussion

Influences of tidal energy advection on the surface energy balance

J. G. Barr et al.

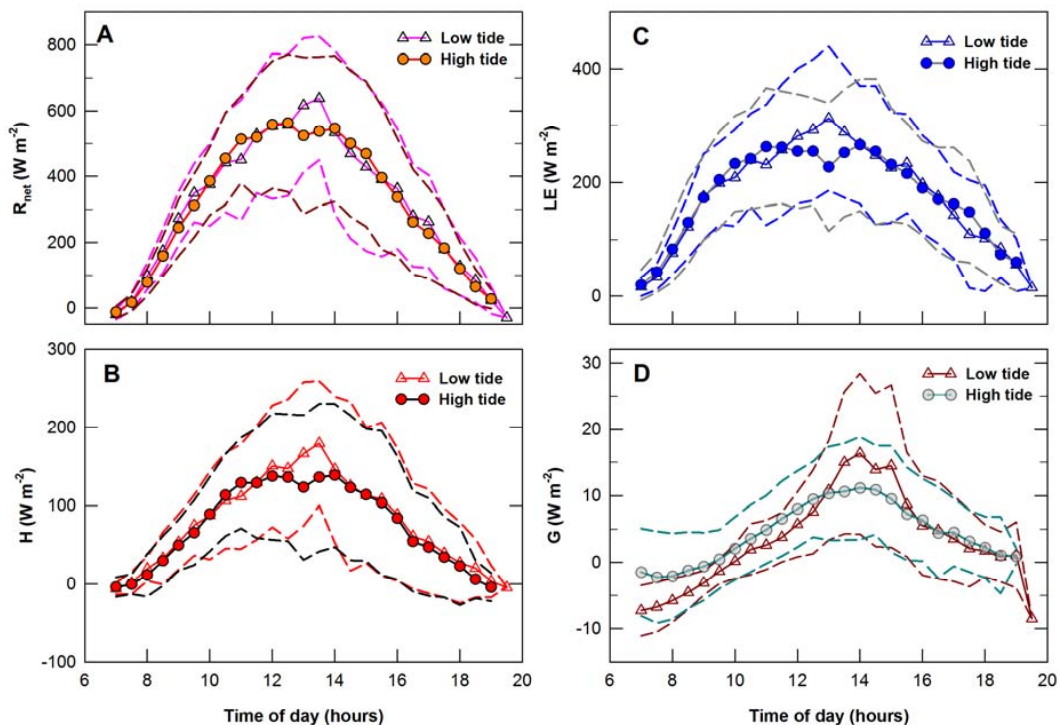


Fig. 4. Half-hourly averages (solid lines) and ± 1 s.d. (dashed lines) of net radiation (R_{net} ; **A**), sensible (H ; **B**) and latent (LE; **C**) heat fluxes, and soil heat flux (G ; **D**) during July to September 2004 and July to August 2005. Flux data were partitioned into periods when the sediment was exposed (low tide) and when the surface was inundated (high tide).

[Title Page](#)
[Abstract](#)
[Introduction](#)
[Conclusions](#)
[References](#)
[Tables](#)
[Figures](#)
[◀](#)
[▶](#)
[◀](#)
[▶](#)
[Back](#)
[Close](#)
[Full Screen / Esc](#)
[Printer-friendly Version](#)
[Interactive Discussion](#)

Influences of tidal energy advection on the surface energy balance

J. G. Barr et al.

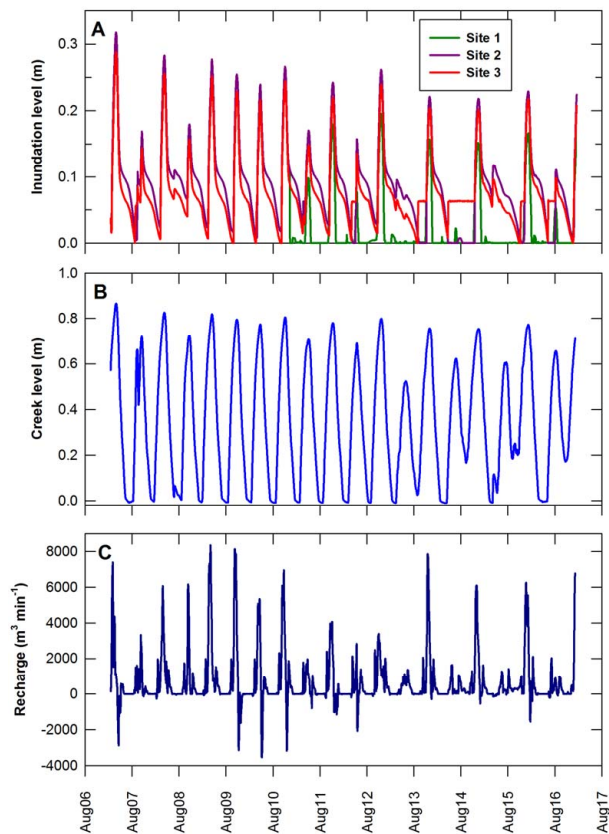


Fig. 5. Water levels inundating the mangrove forest at three sites (Fig. 2) along a transect (A) and within the mouth of the tidal creek (B). Recharge at the mouth of the tidal creek (C) showing flow into the forest (recharge > 0) during flood tide and drainage (recharge < 0) into Shark River during ebb tides.

[Title Page](#)[Abstract](#)[Introduction](#)[Conclusions](#)[References](#)[Tables](#)[Figures](#)[◀](#)[▶](#)[◀](#)[▶](#)[Back](#)[Close](#)[Full Screen / Esc](#)[Printer-friendly Version](#)[Interactive Discussion](#)

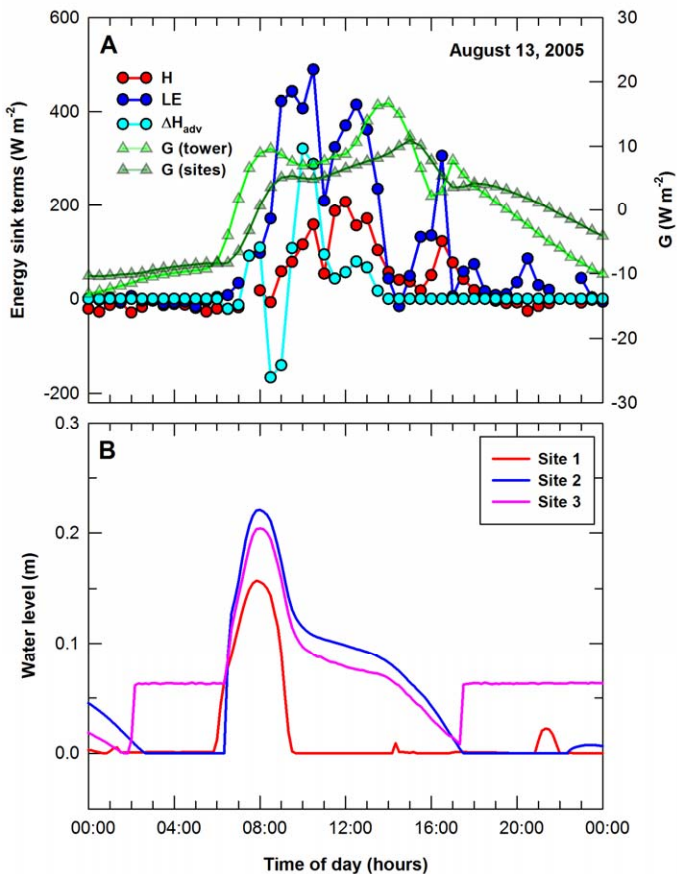


Fig. 6. Diurnal patterns in sensible (H) and latent (LE) heat fluxes, tidal advection of energy (ΔH_{adv}), and soil heat fluxes (G) adjacent to the tower and averaged across the 3 sites (A) and water level trends at the 3 sites (B) on 13 August 2005.

Influences of tidal energy advection on the surface energy balance

J. G. Barr et al.

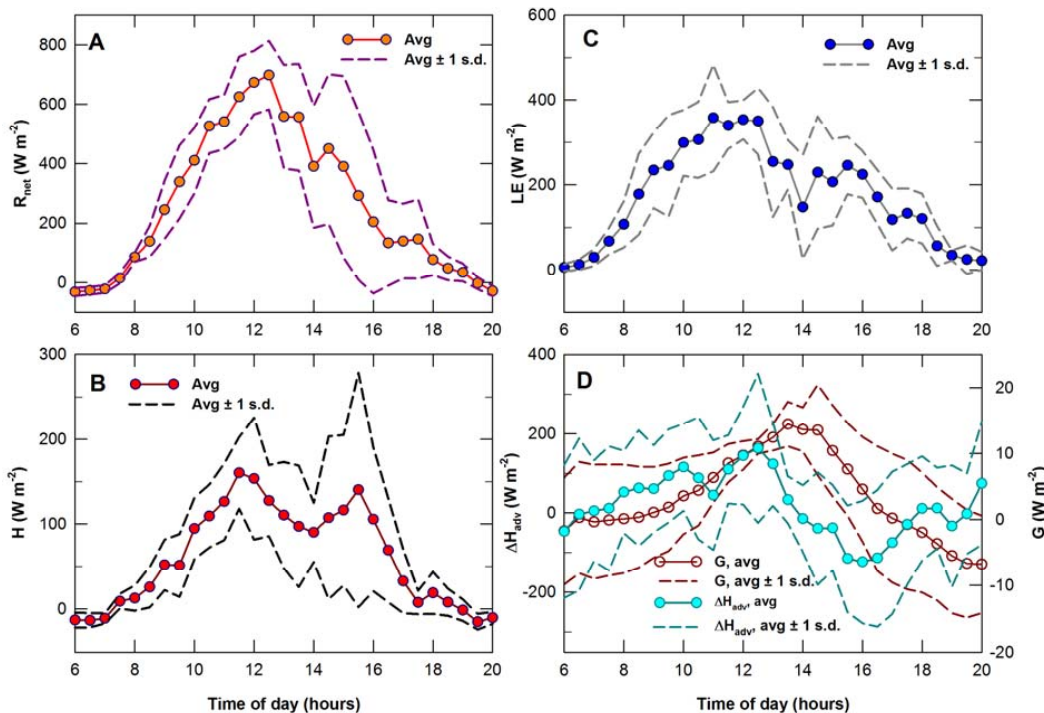


Fig. 7. Diurnal average ± 1 standard deviation (s.d.) of net radiation (R_{net} ; **A**), sensible (H ; **B**) and latent (LE; **C**) heat fluxes, and tidal energy advection (ΔH_{adv} ; **D**) with soil heat flux adjacent to the tower (G ; **D**).

Title Page

Abstract

Introduction

Conclusions

References

Tables

Figures

◀

▶

◀

▶

Back

Close

Full Screen / Esc

Printer-friendly Version

Interactive Discussion



Influences of tidal energy advection on the surface energy balance

J. G. Barr et al.

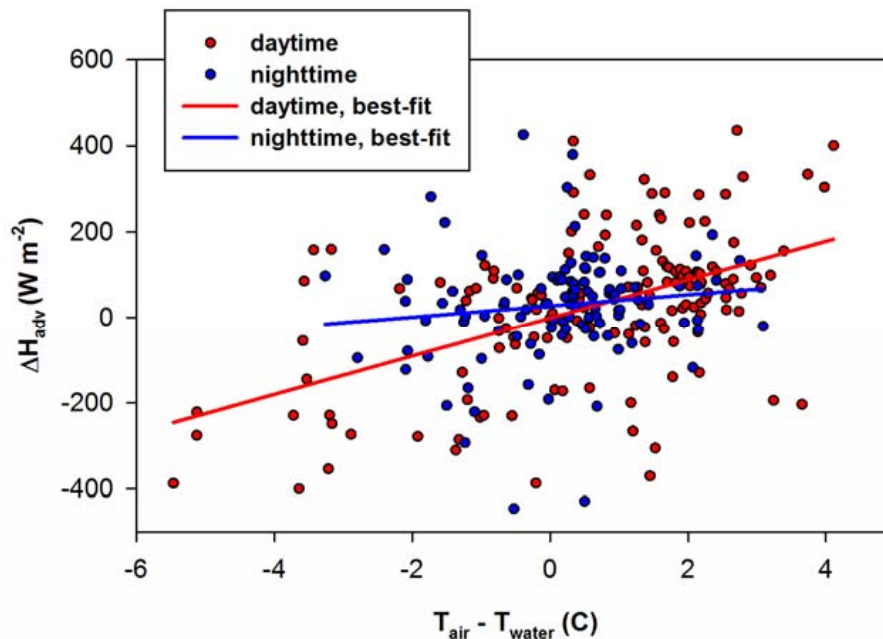


Fig. 8. Daytime and nighttime energy advection (ΔH_{adv} ($W m^{-2}$)) trends as a function of the temperature difference between air temperature (T_{air} ($^{\circ}C$)) at 27 m and depth and site averaged water temperature (T_{water} ($^{\circ}C$)). Least squares regressions were also provided during daytime (slope = 44.7, intercept = -1.4 , $R^2 = 0.25$) and nighttime periods (slope = 13.1, intercept = 26.9, $R^2 = 0.01$).

[Title Page](#)[Abstract](#)[Introduction](#)[Conclusions](#)[References](#)[Tables](#)[Figures](#)[⏪](#)[⏩](#)[◀](#)[▶](#)[Back](#)[Close](#)[Full Screen / Esc](#)[Printer-friendly Version](#)[Interactive Discussion](#)

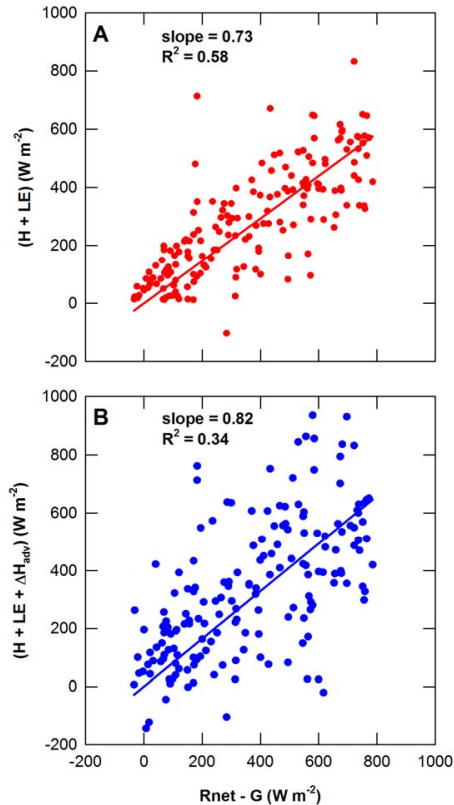


Fig. 9. Half-hourly energy closure during 6–16 August 2005 including only daytime periods without (A) tidal energy advection (ΔH_{adv}) and including it (B). Available energy is the difference between net radiation (R_{net}) and heat flux into the soil (G). Energy output was determined as the sum of sensible (H) and latent (LE) heat fluxes (A) and the sum of H , LE, and tidal energy advection (B). Energy closure improved from 73% (A) to 82% (B) when ΔH_{adv} was added to the energy output.

Influences of tidal energy advection on the surface energy balance

J. G. Barr et al.

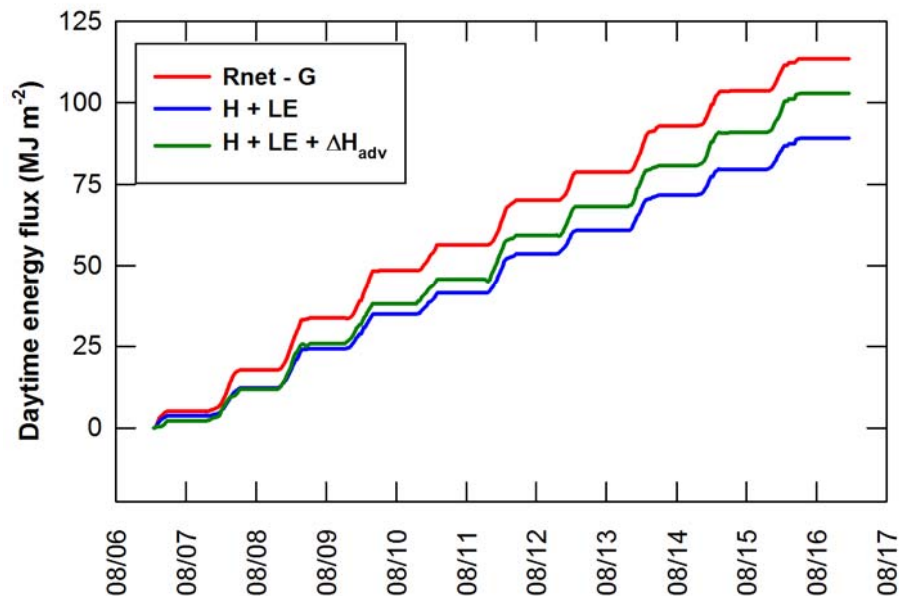


Fig. 10. Cumulative available energy ($R_{\text{net}} - G$) and energy output not including and including energy advection by tides ($[H + LE]$ and $[H + LE + \Delta H_{\text{adv}}]$, respectively) during daytime periods only.

Title Page

Abstract

Introduction

Conclusions

References

Tables

Figures

◀

▶

◀

▶

Back

Close

Full Screen / Esc

Printer-friendly Version

Interactive Discussion

